

## Real-time monitoring of electrically evoked catecholamine signals in the songbird striatum using *in vivo* fast-scan cyclic voltammetry



Amanda R. Smith\*, Paul A. Garris, Joseph M. Casto

School of Biological Sciences, Illinois State University, Campus Box 4120, Normal, IL 61790-4120, USA

### ARTICLE INFO

#### Article history:

Received 20 January 2015

Received in revised form 4 April 2015

Accepted 4 April 2015

Available online 18 April 2015

#### Keywords:

Dopamine

Norepinephrine

European starling

### ABSTRACT

Fast-scan cyclic voltammetry is a powerful technique for monitoring rapid changes in extracellular neurotransmitter levels in the brain. *In vivo* fast-scan cyclic voltammetry has been used extensively in mammalian models to characterize dopamine signals in both anesthetized and awake preparations, but has yet to be applied to a non-mammalian vertebrate. The goal of this study was to establish *in vivo* fast-scan cyclic voltammetry in a songbird, the European starling, to facilitate real-time measurements of extracellular catecholamine levels in the avian striatum. In urethane-anesthetized starlings, changes in catecholamine levels were evoked by electrical stimulation of the ventral tegmental area and measured at carbon-fiber microelectrodes positioned in the medial and lateral striata. Catecholamines were elicited by different stimulations, including trains related to phasic dopamine signaling in the rat, and were analyzed to quantify presynaptic mechanisms governing exocytotic release and neuronal uptake. Evoked extracellular catecholamine dynamics, maximal amplitude of the evoked catecholamine signal, and parameters for catecholamine release and uptake did not differ between striatal regions and were similar to those determined for dopamine in the rat dorsomedial striatum under similar conditions. Chemical identification of measured catecholamine by its voltammogram was consistent with the presence of both dopamine and norepinephrine in striatal tissue content. However, the high ratio of dopamine to norepinephrine in tissue content and the greater sensitivity of the carbon-fiber microelectrode to dopamine compared to norepinephrine favored the measurement of dopamine. Thus, converging evidence suggests that dopamine was the predominate analyte of the electrically evoked catecholamine signal measured in the striatum by fast-scan cyclic voltammetry. Overall, comparisons between the characteristics of these evoked signals suggested a similar presynaptic regulation of dopamine in the starling and rat striatum. Fast-scan cyclic voltammetry thus has the potential to be an invaluable tool for investigating the neural underpinnings of behavior in birds.

© 2015 Elsevier B.V. All rights reserved.

### Introduction

The catecholamines (CA), dopamine (DA) and norepinephrine (NE), are important neuromodulators of many behavioral processes. Current theory suggests that DA encodes the incentive salience of external stimuli (Berridge and Robinson, 1998; Maney, 2013); in effect, DA signals the desirability or value of a stimulus, learned or innate, according to an individual's existing internal state. NE, conversely, is believed to underlie arousal and the allocation of attention (Berridge, 2008), and thus plays a role in the types and identity of stimuli an individual considers salient.

A major limitation in the study of the behavioral neuroscience of these neuromodulators is the difficulty in characterizing their underlying changes during rapid behavioral events. Classical means of monitoring neurochemistry typically involve quantification of the analyte of interest either post-mortem (*via* tissue-punch; Svec et al., 2009; Banerjee et al., 2013) or on the minute time scale in extracellular fluid (*via* microdialysis; Watson et al., 2006), which limits temporal resolution. While these techniques are appropriate for many types of behavioral studies, the use of a real-time neurochemical monitoring technique, such as fast-scan cyclic voltammetry (FSCV), is a valuable complement to these more traditional methods. FSCV provides exquisite temporal and chemical resolution to neurochemical monitoring, and when combined with use of a carbon-fiber microelectrode (CFM), also imparts excellent spatial resolution (Robinson et al., 2008). These characteristics make FSCV at a CFM an excellent tool for *in vivo*

\* Corresponding author. Tel.: +1 309 438 2694.  
E-mail address: [arsmith@ilstu.edu](mailto:arsmith@ilstu.edu) (A.R. Smith).

measurement of behaviorally relevant, subsecond changes in extracellular CA levels. Indeed, *in vivo* FSCV has been used extensively in rat models to characterize behaviorally associated transient changes in DA (Day et al., 2007; Flagel et al., 2011; Gan et al., 2010; Roitman et al., 2008; Willuhn et al., 2014) and to a lesser extent, NE (Park et al., 2012, 2013), but, to our knowledge, has never been used within an intact, non-mammalian vertebrate.

While the value of conventional rodent models is undeniable, at times, alternative natural model organisms are desirable. For example, avian models are particularly tractable for the study of a variety of neural processes, such as vocal learning (Doupe et al., 2005), visual processing (Rogers, 1998), auditory perception and discrimination (Theunissen and Shaevitz, 2006), imprinting (Bolhuis and Honey, 1998), and social behavior (Ball et al., 2002; Goodson and Kingsbury, 2013; O'Connell and Hofmann, 2011). Recently, the actions of DA and NE in these processes have generated considerable interest (Kubikova and Košťál, 2010; Maney, 2013; Riters, 2011). As a starting point for using the strategy of real-time neurochemical monitoring to address these and related processes, the goal of the present study was to establish the use of *in vivo* FSCV in a songbird, the European starling (*Sturnus vulgaris*), to measure electrically evoked CA signals in the avian brain and to compare these measurements to similar *in vivo* measurements in a well-characterized rat model.

To accomplish this, immunohistochemistry was first used to delineate the striatal complex in European starlings and determine stereotaxic coordinates for electrically activating ascending CA neurons. Based on these coordinates, CFMs were inserted into the medial striatum (MSt), which contains the song-learning nucleus Area X, and the lateral striatum (LSt). A stimulating electrode was inserted into the ventral tegmental area (VTA). Electrical stimulation of the VTA evoked signals that were measured at the CFM and identified by the voltammogram of FSCV as CA. These evoked signals were further analyzed to quantify CA release and uptake, and examined for inter-regional differences in presynaptic regulation of extracellular CA. Finally, monoamine content from different striatal regions was examined to determine the relative ratio of DA and NE in striatal tissue of the starling. The avian striatum, like the mammalian striatum, has DA as its primary CA (Juorio and Vogt, 1967; Versteeg et al., 1976); however, in contrast to the mammalian striatum, the avian striatum contains a more prominent NE innervation throughout much of its extent (Kitt and Brauth, 1986a). Because FSCV is unable to distinguish between DA and NE (Baur et al., 1988), the relative contribution of each to the measured signal cannot be directly determined by the voltammogram—as such, the evoked response is initially and conservatively referred to simply as “CA”. This study, establishing *in vivo* FSCV at a CFM for the measurement of electrically evoked CA signals in the striatum of the anesthetized starling, is the necessary first step toward the long-term objective of using the strategy of real-time neurochemical monitoring for assessing brain-behavior relationships in birds.

## Methods

### Animals

For all experiments on birds described below, adult male and female free-living European starlings were captured using potter traps (pedal-activated traps) at our field site in Lexington, Illinois, USA. The birds were maintained in the Illinois State University indoor aviary on a 10:14 (L:D) light cycle at a controlled temperature, and received food and water *ad libitum*. For experiments on rats, male Sprague-Dawley rats were purchased from Harlan Industries (Indianapolis, IN, USA). The rats were housed in the Illinois State University mammalian vivarium with controlled lighting and temperature, and food and water were available *ad libitum*. Experiments were typically performed on rats aged 2–3 months (300–350 g). All animal care and use was in accordance with prevailing local and federal standards and approved by the Institutional Animal Care and Use Committee of Illinois State University.

### Immunohistochemistry

European starlings ( $n = 9$ ; 4 males, 5 females) were euthanized, either in a CO<sub>2</sub> chamber or with an overdose of urethane, and transcardially perfused with heparinized phosphate-buffered saline (PBS) followed by 4% paraformaldehyde. The brains were extracted and post-fixed overnight in 4% paraformaldehyde, and then transferred to a 30% sucrose solution for 2–3 days for cryoprotection. Brains were sectioned at 40  $\mu\text{m}$  on a sliding microtome equipped with a freezing stage and collected into PBS. At a sampling interval of 160  $\mu\text{m}$ , sections underwent immunohistochemistry against dopamine-and-adenosine-related phosphotase-32 (DARPP-32) or tyrosine hydroxylase (TH). The sections were processed using a commercially available kit (VECTASTAIN no. PK-6200, Vector Labs, Burlingame, CA, USA) and were prepared according to manufacturer's instruction except as described. Brain sections were serially rinsed in PBS (3 times, 10 min each); 3% H<sub>2</sub>O<sub>2</sub> for 10 min; PBS, 3 times for 10 min; Vector blocking serum and 0.2% Triton X-100 for 30 min; and incubated overnight at 4 °C with the primary antibody (anti-DARPP-32, 1:3000, Abcam no. ab40801, Cambridge, MA, USA or anti-TH, 1:3000, Immunostar no. 22941, Hudson, WI, USA) and 0.5% Triton X-100. The following day, sections were rinsed in PBS, 3 times for 10 min; Vector secondary antibody and 0.6% Triton X-100 for 30 min; PBS, 3 times for 10 min; Vector ABC reagent and 0.6% Triton X-100 for 30 min; PBS, 3 times for 10 min; 0.05% DAB and 0.015% H<sub>2</sub>O<sub>2</sub> in PBS for 5 min; and again rinsed with PBS. Sections were float-mounted onto chrome alum-subbed slides, allowed to air-dry overnight, dehydrated using a series of alcohol rinses, and coverslipped with Permount. Sections adjacent to immunohistochemistry-stained sections were Nissl-stained to provide detail of nearby cytoarchitecture. Sections undergoing Nissl-staining were float mounted onto chrome alum-subbed slides, allowed to air-dry overnight, rehydrated and stained for 5 s in 1% thionin, dehydrated using a series of alcohol rinses, and coverslipped with Permount. Photomicrographs were taken using a CCD camera (Leica DFC300 FX, Leica Microsystems, Wetzlar, Germany) mounted on a dissecting microscope (Leica MZ95, Leica Microsystems, Wetzlar, Germany). Brightness and contrast were adjusted during image preparation (Photoshop X, Adobe Systems Inc., San Jose, CA, USA) to improve image clarity.

### Determination of stereotaxic coordinates

Because no published stereotaxic atlas of the starling brain existed, initial stereotaxic coordinates for the MSt, LSt and VTA were generated before measurements with FSCV were attempted. Starlings ( $n = 13$  males) were euthanized with CO<sub>2</sub>, exsanguinated, transcardially perfused with heparinized PBS followed by 4% paraformaldehyde, and then decapitated. The head was secured in a stereotaxic frame equipped with a small bird adapter (Kopf no. 914, Tujunga, CA, USA; beak angle at 22°, beak plate at 4 mm). Using the intersection of the ear bars as an anteroposterior (AP) and mediolateral (ML) zero point, per the methods of Kuenzel and Masson (1988), holes were drilled into the skull at coordinates estimated from Nissl-stained brain sections, and no. 2 stainless steel insect pins (36 mm length, 0.45 mm diameter) were inserted into the brain, and allowed to penetrate the opposite side of the skull. The intact head was then removed from the stereotaxic frame and placed in 4% paraformaldehyde overnight. The following day, the pins were carefully removed and the brain was extracted and placed in 4% paraformaldehyde for an additional 24 h, after which the brain was transferred to 30% sucrose in PBS for 2–3 days. Brains were sectioned at 40  $\mu\text{m}$ , and every fourth section was collected and Nissl-stained. Using a compound light microscope, the pin tracks through the sections were evaluated based upon neuroarchitectural landmarks and comparison to existing songbird brain atlases (Stokes et al., 1974; Nixdorf-Bergweiler and Bischof, 2007).

### Surgery

Birds ( $n = 11$ ; 4 males, 7 females) were anesthetized with 20% urethane (8 mL/kg, i.m.) delivered in 2 doses separated by 30 minutes, and secured in a stereotaxic frame. An incision was made through the scalp, and the skin was retracted to expose the surface of the skull. Holes were drilled into the skull (in accordance with the initial AP and ML coordinates that were previously determined relative to the intersection of the ear bars; see the “Determination of stereotaxic coordinates” section) to accommodate an electrode for electrical stimulation, a reference electrode, and two CFMs. Dorsal-ventral (DV) coordinates were initially estimated from Nissl-stained brain sections and functionally confirmed by successful CA measurement; these are given relative to the surface of the brain. A twisted bipolar stimulating electrode (MS 303/2, Plastics One, Roanoke, VA, USA) was lowered into the rostral VTA (−0.8AP, +0.6ML, −9.5 to −10.8DV), a region of the brain rich with DA-producing cells and known to afferently connect to the MSt and LSt (Kitt and Brauth, 1986b). A CFM was lowered into the MSt (+3.9AP, +1.0ML, −4.5 to −7.5DV) and the LSt (+2.8AP, +4.8ML, −5.0 to −7.0DV). A Ag/AgCl reference electrode was inserted into the superficial contralateral pallidum. After the CFMs were inserted into the dorsal striata, stimulating electrode placement within the VTA was optimized for maximal CA release by slowly lowering the stimulating electrode into the VTA in increments of −0.1 mm DV and monitoring changes in the evoked CA signal. Typically, a small but reliable CA signal can be evoked at the dorsal aspect of the VTA, and this signal increases as the stimulating electrode moves ventrally into the

VTA, presumably due to the recruitment of additional CA neurons. The stimulating electrode was lowered until the CA signal slightly decreased, at which point the stimulating electrode was moved +0.1 mm DV to the previous, optimal position and remained fixed there throughout the remainder of the experiment.

Rats ( $n = 8$  males) were similarly anesthetized with 25% urethane (6 mL/kg, i.p.) delivered in 2 doses separated by 30 min, secured in a stereotaxic frame, and the scalp was retracted. Holes were drilled into the skull to accommodate recording, reference, and stimulating electrodes. Coordinates were determined relative to bregma (AP and ML) and the surface of the brain (DV), according to the atlas of Paxinos and Watson (1986). The stimulating electrode was lowered into the medial forebrain bundle (−4.6AP, +1.4ML, −7.0 to −8.0DV), and a CFM was lowered into the dorsomedial striatum (+1.2AP, +2.8ML, −5.0DV; 6° angle). The reference electrode was inserted into the superficial contralateral cortex, and the position of the stimulating electrode was optimized using the same procedure described above.

#### Voltammetry

The CFM was constructed by aspirating a single carbon fiber, approximately 7  $\mu\text{m}$  in diameter (Cytec Engineering Materials, West Patterson, NJ, USA), into a borosilicate glass capillary tube, and using a micropipette puller (PE-2 Micropipette Puller, Narishige, Japan) to create a tight glass seal. A small amount of bismuth wire was inserted into the open end of the capillary tube, and melted around a length of 26G steel wire to ensure good electrical connectivity between the carbon fiber and the steel wire (Ramsson et al., 2011). Under 30 $\times$  magnification, the exposed carbon fiber was trimmed to approximately 100–150  $\mu\text{m}$  by hand using a scalpel. To improve the quality of the seal, CFMs were dipped for 30 s in epoxy composed of EPON Resin 828 (14 parts *m*-phenylenediamine per 100 parts resin; Miller-Stephanson, Morton Grove, IL, USA). Electrodes were briefly dipped in acetone to remove excess epoxy, and then cured overnight in an 80 °C oven.

Data were collected using a Universal Electrochemical Instrument (University of North Carolina at Chapel Hill, NC, USA) under the control of TH-1 software (ESA, Chelmsford, MA, USA) to perform FSCV. The potential at the CFM was cycled through a linear, triangular waveform from −0.4 to +1.3 to −0.4 V at 400 V/s; all measured potentials were relative to the Ag/AgCl reference electrode. CA signals were electrically evoked using computer controlled stimulus trains of constant current that were optically isolated from the electrochemical system (NL800A, Neurolog, Medical Systems Corp., Great Neck, NY, USA) to prevent stimulation-induced artifacts in voltammetric monitoring. The trains consisted of biphasic stimulation pulses (300  $\mu\text{A}$  and 2 ms each phase) at varying frequencies and train durations. Three stimulus trains were used: 120 pulses at 60 Hz, a supraphysiological stimulation used to evoke a robust CA signal and saturate transporters to support the direct measurement of  $V_{\text{max}}$  for CA uptake from the slope of the clearance of the electrically evoked CA signal (see the “Data analysis” section); 24 pulses at 60 Hz, a reinforcing stimulation in rats (Cheer et al., 2005) producing signals resembling the amplitude and dynamics of naturally occurring phasic DA signals called transients recorded in the striatum of the unanesthetized rat (Robinson et al., 2008) and that are amenable for the analysis of release and uptake parameters (Covey et al., 2014); and 4 pulses at 30 Hz, a physiological stimulation approximating burst firing of midbrain DA neurons recorded in the unanesthetized rat (Hyland et al., 2002). We chose to use stimulation parameters based on those of confirmed DA neurons in the rat, because we know of no similar estimates from confirmed DA neurons in songbirds (but see Yanagihara and Hessler, 2006 for highly variable firing rates of unidentified neurons within the VTA of behaving zebra finches). Catecholamines were identified by the presence of current peaks at 0.6 V and −0.2 V in its background-subtracted voltammogram.

Current amplitude was converted to concentration based on post-calibration for DA using flow injection analysis (Kristensen et al., 1986), which exposed the CFM to a bolus injection of analyte within a flowing stream. A syringe pump (Pump II Pico Plus, Model 70-2213, Harvard Apparatus, Holliston, MA, USA) equipped with a 60 mL syringe was attached to a reservoir through a solenoid and pneumatic actuator (Rheodyne Model 7163, Solenoid Valve Kit, Alltech Associates, Deerfield, IL, USA) that drove an injection port (Rheodyne Model 5712 Low Pressure Switching Valve, Alltech Associates). This allowed the flow to the reservoir to be switched to a specific concentration of analyte (e.g., 1  $\mu\text{M}$  DA, the concentration used for DA post-calibration of each CFM) mid-stream. The CFM was suspended in the buffer-filled (1 $\times$  Tris-buffered saline) reservoir directly above the pump outflow tubing, and buffer was pumped through the system at a rate of 3 mL/min. Because the voltammogram for DA is not reliably distinguishable from that of NE (Baur et al., 1988), and both could contribute to the evoked CA signal measured in the starling striatum with FSCV, a subset ( $n = 6$ ) of CFM were calibrated for DA, then NE, each at concentrations of 0.1  $\mu\text{M}$ , 1  $\mu\text{M}$  and 10  $\mu\text{M}$ . This facilitated assessment of the relative sensitivity of the electrodes to these two electroactive compounds and the likely contributions of each to a composite CA signal.

To assess accuracy of CFM placement, electrolytic lesions were made at the recording sites by lowering a 28G steel wire enclosed in a borosilicate glass capillary tube (with  $\approx 1$  mm protruding) to the appropriate coordinates and applying 10 V with a DC power supply (BK Precision 1710, Chicago, IL, USA) for 10 s. These brains were then extracted and stained for DARPP-32 immunoreactivity, as described in

the “Immunohistochemistry” section. Stimulating electrode placement was also examined. The relatively large size of the stimulating electrode reliably produced a visible electrode track within the VTA and regions located dorsally to it without an electrolytic lesion, and the presence of DA cells at the ventral extent of the electrode track site was confirmed with immunohistochemistry for TH.

#### Determination of monoamine content in the basal forebrain

A subset of post-surgical starlings ( $n = 5$  females) were overdosed with urethane, decapitated, and their brains rapidly extracted. The brains were bisected along the longitudinal fissure, and the left hemisphere was flash-frozen in pulverized dry ice, wrapped in foil, and stored at −80 °C. The hemispheres were cut into 100  $\mu\text{m}$  thick coronal sections on a cryostat (Microm HM 550, Thermo Scientific, Waltham, MA, USA), and 1 mm-diameter tissue punches were taken from the anterior MSt, posterior MSt (defined by the presence of the LSt in the coronal plane of section), the nucleus accumbens (NAc), LSt, Area X, and the hypothalamus (as per Palkovits, 1973). Tissue punch accuracy was assessed by collecting punched sections onto chrome alum-subbed slides and using a Nissl stain (see the “Immunohistochemistry” section) to reveal nearby cytoarchitecture; inaccurate punches were discarded. Monoamine content was determined using high-performance liquid chromatography with electrochemical detection (HPLC-EC) (Pump: ISO-3100BM, Dionex, Pittsburgh, PA, USA; Detector: Choulochem III, Dionex, Pittsburgh, PA, USA) using an analytical, reverse phase column (MD-150, Dionex, Pittsburgh, PA, USA). The mobile phase (pH 3.0), in 2 L water, contained: 20.7 g sodium dihydrogen phosphate monohydrate, 0.735 g 1-octanesulfonic acid sodium salt, 200  $\mu\text{L}$  triethylamine, 25  $\mu\text{M}$  EDTA, and 200 mL acetonitrile. Tissue protein content was determined using a commercially available kit (Bio-Rad, Hercules, CA, USA).

#### Data analysis

Electrically evoked CA signals were analyzed using equations based upon a general model describing the rate of change of extracellular [CA] ( $d[\text{CA}]_{\text{EC}}/dt$ ) as a balance between the opposing rates of CA release and uptake (Wu et al., 2001):

$$\frac{d[\text{CA}]}{dt} = \left\{ \frac{d[\text{CA}]}{dt} \right\}_{\text{release}} - \left\{ \frac{d[\text{CA}]}{dt} \right\}_{\text{uptake}} \quad (1)$$

where  $\{d[\text{CA}]/dt\}_{\text{release}}$  is the CA release rate and  $\{d[\text{CA}]/dt\}_{\text{uptake}}$  is the CA uptake rate. In this model, only the uptake term operates after cessation of the stimulus train (i.e.,  $\{d[\text{CA}]/dt\}_{\text{release}} = 0$ ). Using this general model, two methods of analysis were performed.

The first type of analysis used non-linear regression with simplex minimization to fit measured evoked signals to calculated curves (Wu et al., 2001). This analysis used two different kinetic schemes for CA uptake to calculate curves. The first scheme assumed Michaelis–Menten uptake kinetics (Wightman et al., 1988):

$$\frac{d[\text{CA}]_{\text{EC}}}{dt} = \frac{[\text{CA}]_p \times f - V_{\text{max}}}{K_m / ([\text{CA}] + 1)} \quad (2)$$

where  $[\text{CA}]_p$  is the concentration of CA released per stimulus pulse,  $f$  is the stimulus pulse frequency,  $V_{\text{max}}$  is the maximal rate of CA uptake by its transporter, and  $K_m$  is a constant related to the inverse of the affinity of CA for its transporter(s).  $K_m$  was either allowed to float independently with  $[\text{CA}]_p$  and  $V_{\text{max}}$ , or was fixed. The second scheme assumed pseudo first-order uptake kinetics to calculate curves (Ramsson et al., 2011):

$$\frac{d[\text{CA}]}{dt} = [\text{CA}]_p \times f - k \times [\text{CA}] \quad (3)$$

where  $k$  is the first-order rate constant. Eq. (2) was used to fit CA signals evoked by both 24- and 120-pulse stimulations, while Eq. (3) was restricted to CA signals evoked by 24-pulse stimulations, as CA uptake following 120-pulse stimulations did not approach first-order decay.

The second type of analysis determined release and uptake parameters from linear regions of the electrically evoked CA signals (Wu et al., 2001). Assuming that high [CA], such as that elicited by supraphysiological stimulation, saturates transporters (i.e., CA uptake is pseudo zero-order),  $V_{\text{max}}$  was determined by (Wu et al., 2001):

$$V_{\text{max}} = - \left\{ \frac{d[\text{CA}]}{dt} \right\}_{\text{uptake}} \quad (4)$$

Further assuming that the rate of CA uptake is similar at the same [CA] during stimulation (i.e., upward phase of the evoked signal) and after stimulation (i.e., downward phase of the evoked signal),  $[\text{CA}]_p$  was determined by (Wu et al., 2001):

$$[\text{CA}]_p = \frac{\{d[\text{CA}]/dt\}_{\text{upward}} - \{d[\text{CA}]/dt\}_{\text{downward}}}{f} \quad (5)$$

where  $\{d[\text{CA}]/dt\}_{\text{upward}}$  and  $\{d[\text{CA}]/dt\}_{\text{downward}}$  are the rate of change of [CA] during the upward and downward phase of the electrically evoked CA signals, respectively.

This analysis of  $[CA]_p$  is conceptually based on the notion that both CA release and uptake occur during stimulation but that only CA uptake occurs after stimulation (see Eq. (1) and its description above). Thus, subtracting the rate of change of the downward phase (i.e.,  $-d[CA]/dt_{\text{uptake}}$ ) from the rate of change of the upward phase (i.e.,  $d[CA]/dt_{\text{release}} - d[CA]/dt_{\text{uptake}}$ ) reveals the rate of release. Because this analysis requires saturation of CA transporters, its use was limited to CA signals electrically evoked by the 120-pulse, 60-Hz train.

Data are expressed as mean  $\pm$  SEM, and  $n$  is equal to the number of animals. Data were analyzed using an ANOVA or Student's  $t$ -test, as appropriate (SAS 9, SAS Institute, Cary, NC, USA). In cases where the assumption of normality was not met, data were log-transformed (1 instance) or a Wilcoxon signed-rank test was substituted (1 instance). Sex was initially included as a variable in all analyses on starlings, but because no significant effect due to sex was found for any measure, sex was excluded from the analyses to increase statistical power. Statistical significance was set at  $p < 0.05$ .

## Results

### DARPP-32-immunoreactivity in the starling striatum

Because the overall goal of this study was to establish FSCV for the measurement of electrically evoked CA levels in the striatum of the urethane-anesthetized starling, both recording and stimulating sites were first identified. To accomplish this step, DARPP-32-immunoreactivity (IR), was used to delineate the LSt and MSt, targets for recording CA with FSCV. DARPP-32, a phosphoprotein involved in the regulation of protein phosphatase-1, typically colocalizes with D1 receptors (Walaas and Greengard, 1984) and is considered to be an effective indicator of dopaminergic cells (Durstewitz et al., 1999). Striatal boundaries were determined using the dopaminergic cell marker DARPP-32, rather than the more commonly used catecholaminergic cell marker TH, because DARPP-32 clearly delineates between the dopaminergic MSt and the adjacent noradrenergic lateral bed nucleus of the stria terminalis (BSTL) (Bálint and Csillag, 2007). DARPP-32-IR was dense and fairly uniform throughout the MSt and LSt and exhibited expected regional heterogeneity in the ventral pallidum and globus pallidus (Fig. 1), though DARPP-32-IR was unexpectedly reduced within Area X in comparison to the surrounding MSt. A conspicuous dearth of DARPP-32-IR indicative of the BSTL was located adjacent to the lateral ventricle, beginning as a small region medial to the caudal extent of Area X and then expanding laterally farther posterior.

### Tissue monoamine content

The monoamines, DA, NE and serotonin (5-HT), are all electroactive and amenable to detection with FSCV (Robinson et al., 2008). Tissue monoamine levels in starling striata and other regions of the basal forebrain were therefore quantified with HPLC-EC to assess their relative abundance (Fig. 2). Although among-individual variation in tissue content of the various monoamines was noted, no individual values were more than 2 standard deviations from the mean for any brain region. As a general trend, this analysis found relatively high DA content in Area X and the posterior MSt, followed closely by anterior MSt and nucleus accumbens, but with considerably less in the LSt and as expected very low levels in the hypothalamus. NE content was highest in the hypothalamus followed by the NAc and Area X but similarly low levels in the MSt and LSt. Importantly, there was significantly greater DA than NE content in the two regions where CFM were placed, the anterior MSt ( $p = 0.038$ ) and the LSt ( $p = 0.007$ ).

### Sensitivity of CFM to DA and NE

Although all three monoamines are amenable to detection by FSCV, the voltammogram for 5-HT is readily distinguished from that of both DA and NE (Baur et al., 1988; Jackson et al., 1995;

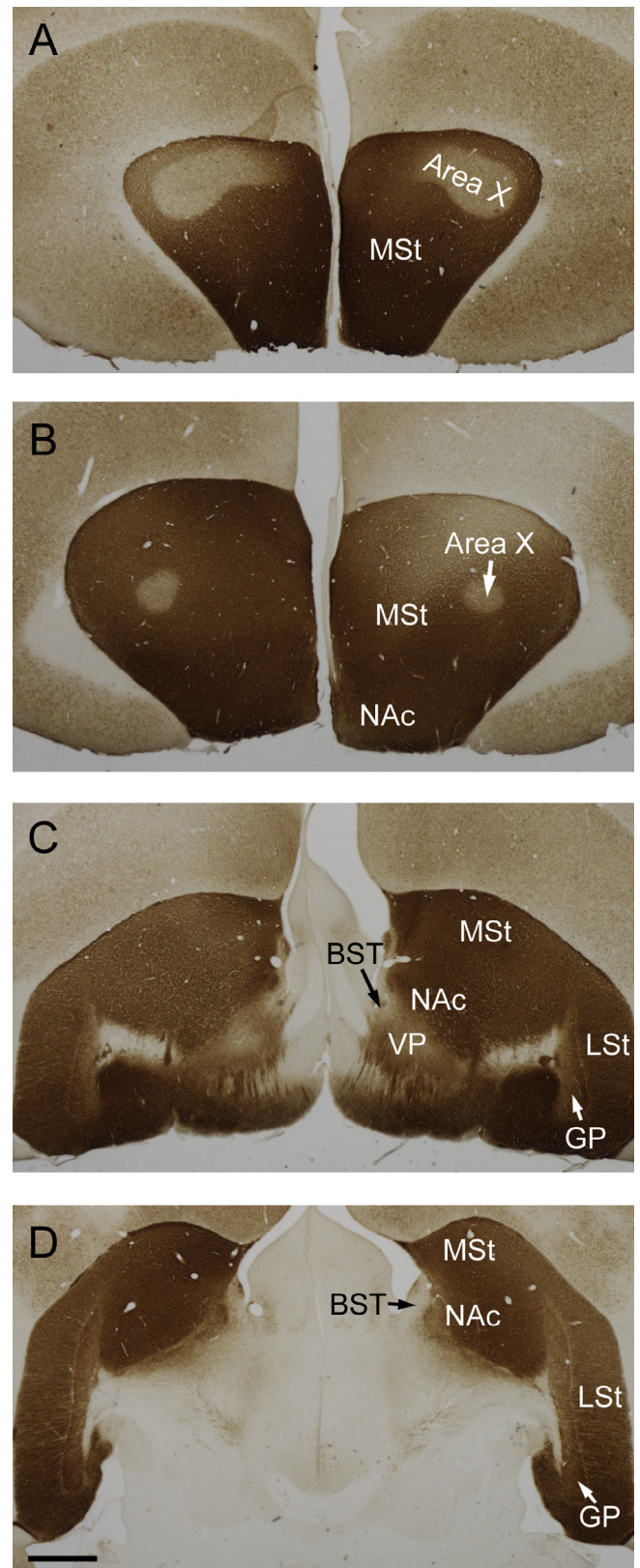


**Fig. 1.** Coronal sections showing DARPP-32-immunoreactivity in a female European starling forebrain. Sections are arranged anterior to posterior, and have a sampling interval of 0.8 mm. Scale bar = 1 mm. Abbreviations: BST, bed nucleus of the stria terminalis; GP, globus pallidus; LSt, lateral striatum; MSt, medial striatum; NAc, nucleus accumbens; VP, ventral pallidum.

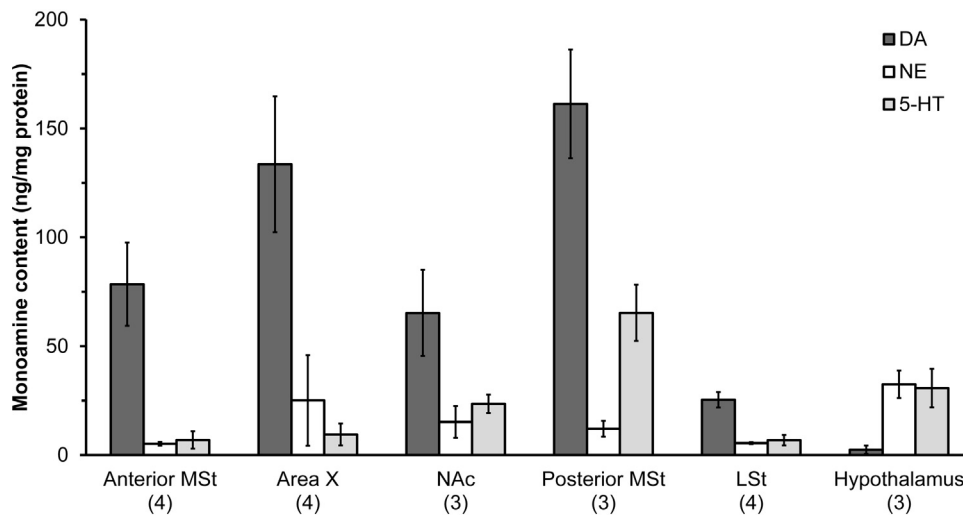


**Fig. 2.** Monoamine content in the starling basal forebrain. Tissue punches were collected from several sub-regions in the starling basal forebrain (sample sizes are given below each region), and monoamine content was determined using HPLC–EC. Data are means  $\pm$  SE. See the Results section for statistical comparisons.

Heien et al., 2003). Thus, if electrically evoked in the starling striatum, 5-HT release would be evident. However, voltammograms for DA and NE are not distinguishable. Because the HPLC–EC analysis of tissue content revealed measureable amounts of both DA and NE in the starling striatum, other criteria must be considered for identifying the CA released. One consideration is that previous work has demonstrated enhanced sensitivity of the CFM, the microsensor used with FSCV, for DA compared to NE (Baur et al., 1988; Gale and Perkel, 2005). Due to a different CFM and FSCV waveform in the present study, it is important to establish the relative sensitivities to DA and NE for the recording conditions to be used in the starling striatum. Fig. 3 shows voltammograms (Fig. 3A) and calibration curves (Fig. 3B) for such conditions. While there is considerable overlap between voltammograms for DA and NE, the CFM exhibits a  $>2$ -fold greater sensitivity ( $p = 0.008$ ) for DA (20.0 nA/ $\mu$ M) than for NE (8.65 nA/ $\mu$ M), consistent with previous work (Baur et al., 1988; Gale and Perkel, 2005).

$\mu$ M), consistent with previous work (Baur et al., 1988; Gale and Perkel, 2005).

#### Electrically-evoked dopamine dynamics in the starling striatum

Based on the stereotaxic coordinates generated, CFMs were inserted into the anterior MSt and LSt, and a stimulating electrode into the VTA (Fig. 4). Fig. 5 shows exemplar recordings of electrically evoked CA signals elicited by the three stimulus trains used in the present study (Fig. 5A: 24 pulses at 60 Hz; Fig. 5B: 4 pulses at 30 Hz; Fig. 5C: 120 pulses at 60 Hz). All three trains resulted in a sharp increase or “spike” of CA measured with FSCV at the CFM that rapidly returned to baseline. Associated voltammograms, whether plotted individually in Insets or sequentially in color plots above each recording, showed an oxidation peak at  $\approx +0.6$  V and a reduction peak at  $\approx -0.2$  V, which is characteristic of

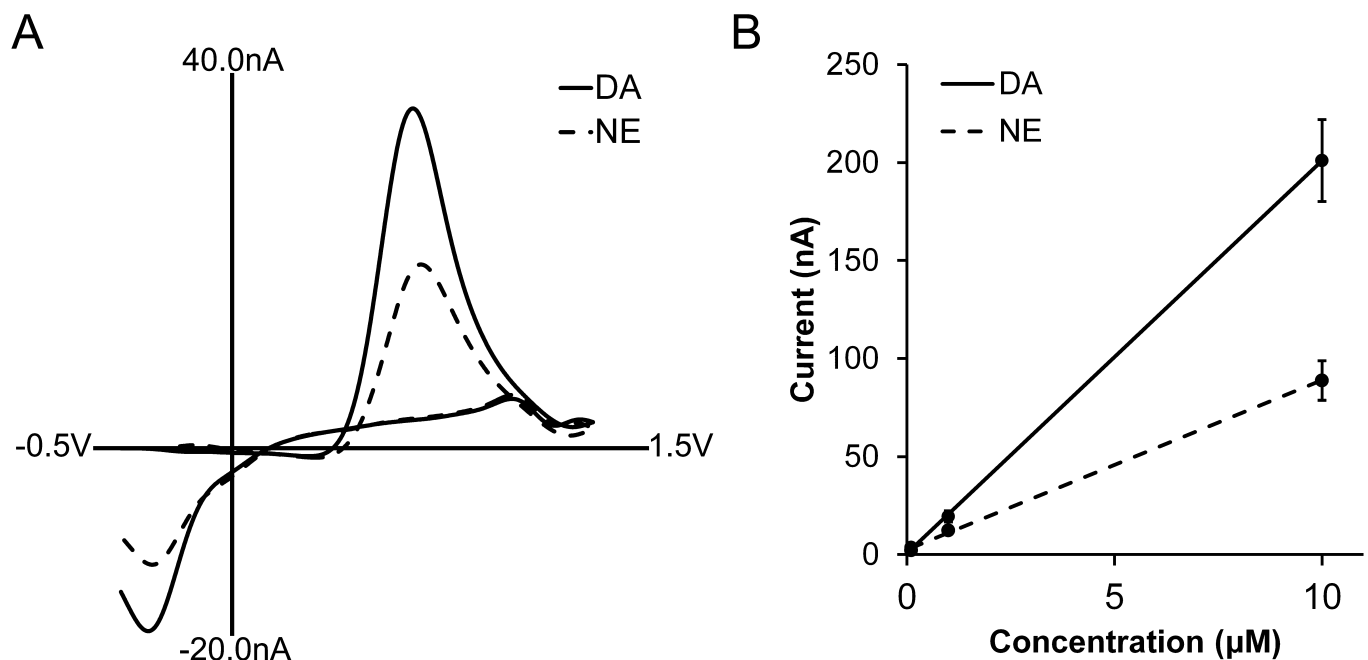


**Fig. 3.** Comparison of CFM sensitivity for DA versus NE. Currents generated by DA and NE were measured during flow injection analysis. (A) Background-subtracted cyclic voltammograms generated by 1- $\mu$ M DA or NE ( $n = 3$  CFMs). (B) Currents measured from boluses of 0.1  $\mu$ M, 1  $\mu$ M, and 10  $\mu$ M DA or NE. Data are means  $\pm$  SE. ( $n = 3$  CFMs). In some cases where the error magnitude is small, the bars are obscured by the symbols.

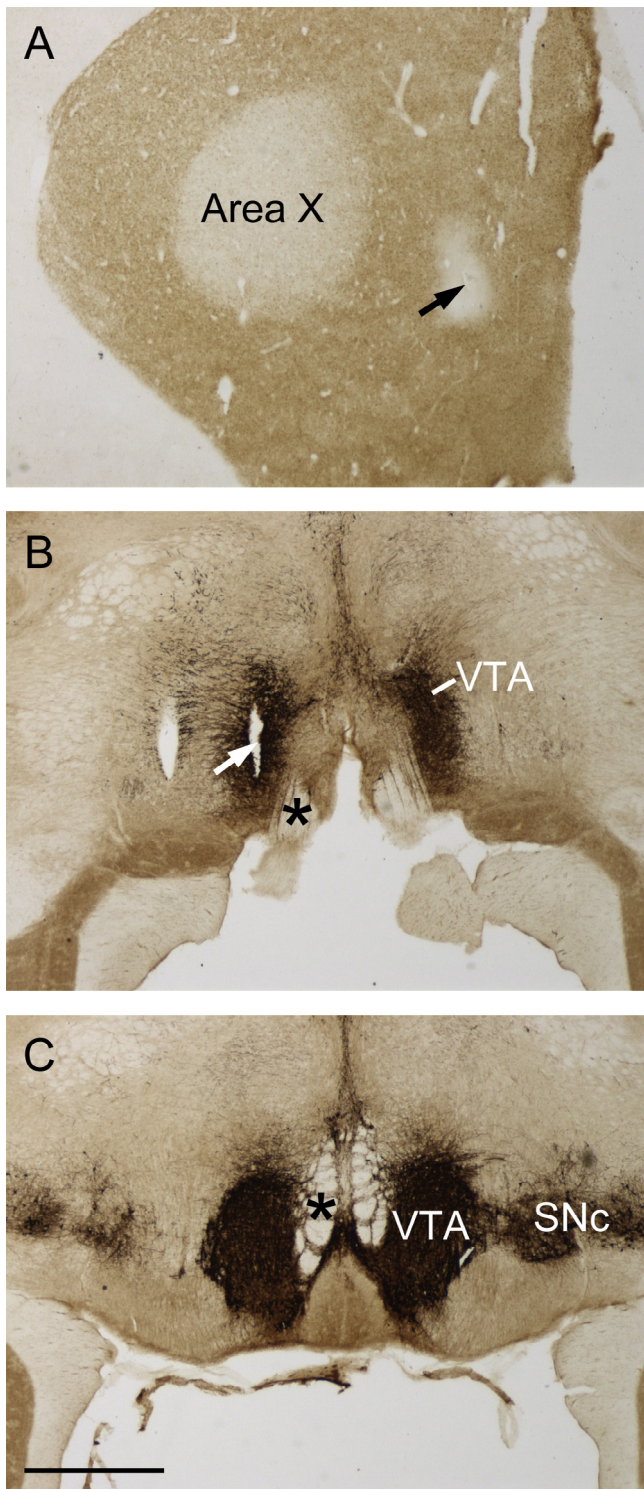


**Fig. 4.** Histological confirmation of electrode locations in a male starling. (A) DARPP-32-immunoreactive coronal brain section confirming a successful recording of CA in the starling MST. A steel wire lowered to the coordinates of the CFM was used to create a small burn (located at the tip of the arrow) at the recording site. An oblong corona of reduced immunoreactivity surrounds the burn. (B–C) Coronal brain sections at the level of the anterior (B) and posterior (C) VTA exhibiting TH immunoreactivity. Arrow indicates lesion from one pole of the electrode penetrating the anterior VTA, confirming stimulating electrode placement. Note that the stimulating electrode was placed approximately 0.5 mm rostral to the anteriormost extent of the SNc. Asterisk indicates the location of the oculomotor nerve in relation to the VTA. Scale bar = 1 mm. Abbreviations: SNc, substantia nigra pars compacta; VTA, ventral tegmental area.

both DA and NE (Baur et al., 1988). Average values for the maximal concentration of CA ( $[CA]_{max}$ ) elicited by each stimulus train are shown in Table 1.

To better characterize the anatomical target for activating CA neurons ascending to the MST, we investigated the effect of stimulating electrode position on electrically evoked CA signals. Throughout this experiment, we stimulated the VTA with the 24-pulse, 60-Hz train. We held the CFM stationary in the anterodorsal MST and incrementally lowered the stimulating electrode ventrally into the VTA. We found that  $[CA]_{max}$  tended to peak when the stimulating electrode was approximately 10–10.5 mm below the brain surface, and began to decline again as the electrode continued to move more ventrally (Fig. 6). This pattern presumably corresponds to the stimulating electrode descending ventrally into, and eventually through, the VTA. These results are consistent with the effect, on striatal DA release, of lowering the stimulating electrode through the VTA–SNc region of the rat (Garris et al., 1993) and the medial forebrain bundle (MFB) in the rat (Garris et al., 1993) and Syrian hamster (Greco et al., 2006). As illustrated by the Insets in Fig. 6, although  $[CA]_{max}$  changed during lowering of the stimulating electrode, electrically evoked CA dynamics did not, suggesting that the same neurochemical species was elicited and the same neuron type(s) was activated at each depth.

To similarly characterize the anatomical target for measuring electrically evoked CA levels in the starling striatum, we then investigated the heterogeneity of CA release sites across the MST by modifying CFM placement along a dorsal–ventral trajectory, while holding the position of the stimulating electrode constant within the VTA. Similar to the striatum of the rat (Garris et al., 1994) and hamster (Greco et al., 2006), there is marked heterogeneity with regard to CFM depth and  $[CA]_{max}$  electrically evoked by the 24-pulse, 60-Hz train. We also found an overall tendency for  $[CA]_{max}$  to decline as the CFM was moved ventrally (Fig. 7), but this pattern was not statistically significant ( $r^2 = 0.230$ ). Again, while  $[CA]_{max}$  varied with CFM depth, electrically evoked CA dynamics did not (see insets in Fig. 7), suggesting that the same neurochemical species was elicited at each recording location.

#### Presynaptic regulation of [CA] in the starling striatum

In their respective terminal fields of the rat brain, extracellular concentrations of DA and NE are tightly regulated by the presynaptic mechanisms of exocytotic release and neuronal uptake (Capella et al., 1993; Mitchell et al., 1994; Garris and Wightman, 1994). Parameters describing these mechanisms for release and uptake can be quantified from electrically evoked signals measured by voltammetry and CFMs (see the Data analysis section; Wightman et al., 1988; Wu et al., 2001). Collectively, this analysis has found regionally distinct presynaptic control for both DA and NE that is associated with different functions for the two neuromodulators (Mitchell et al., 1994; Garris and Wightman, 1994). We therefore performed a similar analysis of CA release and uptake in the starling striatum.

In the first analysis, signals electrically evoked by the 24-pulse, 60-Hz train were fit to a general model describing the rate of change of [CA] as a balance of opposing CA release and uptake rates (Wu et al., 2001). This stimulus train was selected because it produces phasic-like DA responses in the rat striatum mimicking naturally occurring DA transients (Covey et al., 2014), and because these responses are amenable to curve fitting using non-linear regression for determining parameters for DA release and uptake (Ramsson et al., 2011; Daberkow et al., 2013). In contrast, signals evoked by the 4-pulse, 30-Hz stimulation are too small for accurate fitting without additional higher DA signals (Howard et al., 2011), and signals evoked by the suprphysiologically 120-pulse, 60-Hz

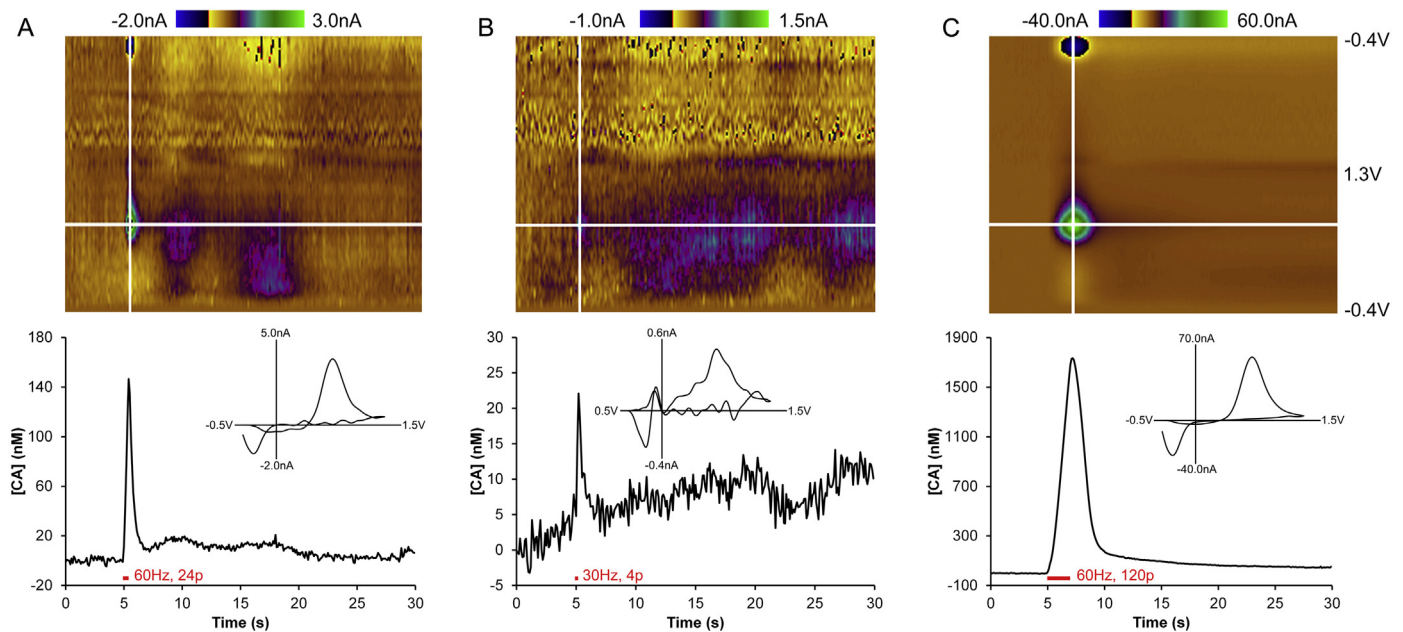


**Fig. 5.** Exemplar traces of electrically evoked extracellular CA signals recorded using FSCV in the MST of a female starling. Each trace employed a different stimulation regimen (specified in red text). (top, A–C) Color plots serially displaying background-subtracted voltammograms ( $x$  axis—time;  $y$  axis—applied potential;  $z$  axis—measured current). (bottom, A–C) Electrically evoked CA dynamics measured at peak oxidative potential for DA. Each plot corresponds to the horizontal white line in the corresponding color plot above. Red bars indicate electrical stimulus duration. (inset, A–C) Individual background-subtracted cyclic voltammogram determined from the signal peak, confirming chemical identity as CA. Each voltammogram corresponds to the vertical white line in the corresponding color plot above. (For interpretation of the references to color in this figure legend, the reader is referred to the web version of this article.)

stimulation require additional low-frequency responses for accurate fitting (Wu et al., 2001). Table 2 shows CA release and uptake parameters determined for starling striata with stimulation of the VTA. Assuming Michaelis–Menten uptake kinetics,  $[CA]_p$  was significantly greater in the LSt than in the MST ( $p = 0.032$ ), while no significant differences were found in  $V_{max}$  ( $p = 0.678$ ) and  $K_m$  ( $p = 0.344$ ) between the striatal regions.

Because determination of  $K_m$  for uptake is difficult *in vivo* (Wu et al., 2001), additional analyses were conducted to further investigate CA release and uptake in the starling striatum. Responses evoked by the 24-pulse, 60-Hz trains were additionally fit to the general model using non-linear regression but assuming first-order uptake kinetics. Consistent with the analysis of CA uptake assuming Michaelis–Menten kinetics, and also shown in Table 2, CA uptake as characterized by  $k$  was similar in the two striatal regions, and  $[CA]_p$  was significantly greater in the LSt as compared to the anterior MST ( $p = 0.032$ ). Similar values of CA release and uptake between the two analyses support the determination of  $K_m$ . CA signals evoked in the starling striata by the supraphysiological stimulation (120-pulse, 60-Hz train) were also assessed for CA release and uptake. The high  $[CA]$  of these evoked signals permits a unique analysis based on slopes, and these results can be compared to analysis of the same evoked signals with non-linear regression after fixing  $K_m$  to the values determined above (MST  $K_m = 270$  nM, LSt  $K_m = 360$  nM). As shown in Table 3, there was no significant difference between  $V_{max}$

( $p = 0.770$ ) or  $[CA]_p$  ( $p = 0.583$ ) as calculated using the slopes method or non-linear regression analysis. Additionally,  $[CA]_p$  ( $p = 0.836$ ) and  $V_{max}$  ( $p = 0.194$ ) did not significantly differ between the anterior MST and LSt.

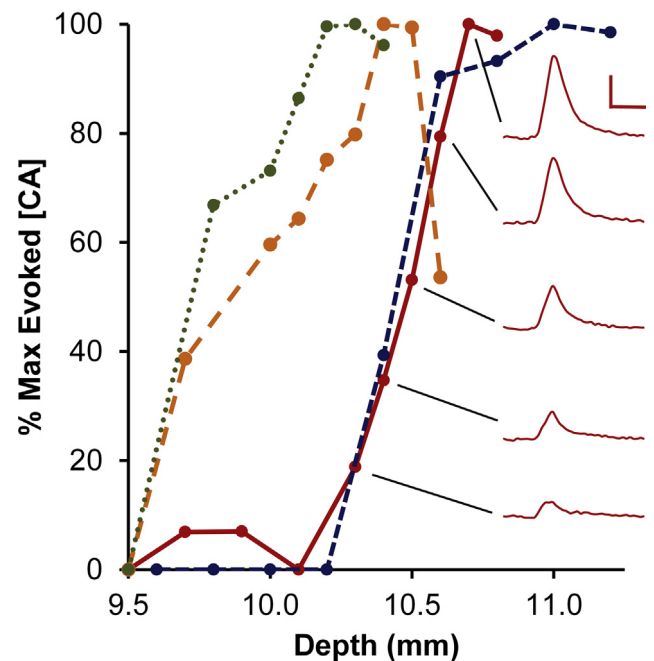


**Fig. 6.** Effect of stimulating electrode depth on the maximal amplitude ( $[CA]_{max}$ ) of the electrically evoked CA signal. Each line represents data from a different individual. For all measurements, the CFM was located in a single location in the dorsal MST throughout the procedure. The stimulating electrode was lowered incrementally into the VTA. Stimulating electrode depth is relative to the brain surface. (Insets) Representative traces from a single starling (red line) depicting changes in  $[CA]_{max}$  in conjunction with stimulating electrode depth. Horizontal scale bar = 1 s, vertical scale bar = 100 nM. (For interpretation of the references to color in this figure legend, the reader is referred to the web version of this article.)

**Table 1**  
 $[CA]_{max}$  elicited by different stimulation parameters (mean  $\pm$  SE).

	$[CA]_{max}$ (nM)		
	30 Hz, 4p	60 Hz, 24p	60 Hz, 120p
Starling			
Lateral striatum	34 $\pm$ 7	330 $\pm$ 77	2296 $\pm$ 380
Medial striatum	21 $\pm$ 2	256 $\pm$ 37	1945 $\pm$ 365
Rat			
Dorsomedial striatum	–	340 $\pm$ 78	–

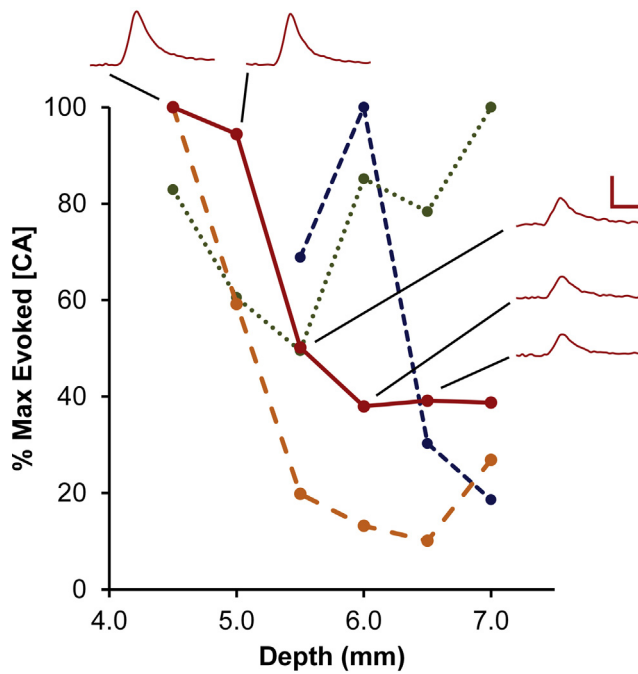


**Fig. 7.** Effect of CFM depth on the maximal amplitude ( $[CA]_{max}$ ) of the electrically evoked CA signal. Each line represents data from a different individual. For all measurements, the stimulating electrode was located in a single location in the VTA throughout the procedure. The CFM was lowered incrementally ( $-0.5$  DV per measurement) through the MSt. CFM depth is relative to the brain surface. (Insets) Representative traces from a single starling (red line) depicting changes in  $[CA]_{max}$  in conjunction with CFM depth. Horizontal scale bar = 1 s, vertical scale bar = 100 nM. (For interpretation of the references to color in this figure legend, the reader is referred to the web version of this article.)

#### Presynaptic regulation of [DA] in the rat striatum

FSCV at a CFM is well established in the rat for measuring extracellular DA in the striatum electrically evoked by stimulation of ascending DA axons (Stamford, 1990). Converging evidence in rats suggests that these evoked signals are attributable to DA rather than NE, including higher sensitivity of the CFM for DA versus NE (Baur et al., 1988), a  $\approx 50$  to 100-fold difference in DA versus NE tissue content (Garris et al., 1993), selectivity in

**Table 2**  
Comparison of parameters for CA release and uptake determined from signals evoked by the 24-pulse, 60-Hz train in starling and rat striata (mean  $\pm$  SE).

	Michaelis–Menten kinetics			Pseudo-first order kinetics	
	$V_{max}$ (nM/s)	$[CA]_p$ (nM)	$K_m$ (nM)	$k$ ( $s^{-1}$ )	$[CA]_p$ (nM/s)
Starling					
Lateral striatum	1221 $\pm$ 191	35 $\pm$ 5	359 $\pm$ 70	2.43 $\pm$ 0.44	37 $\pm$ 5
Medial striatum	1291 $\pm$ 190	25 $\pm$ 4	271 $\pm$ 38	2.66 $\pm$ 0.25	25 $\pm$ 4
Rat					
Dorsomedial striatum	1103 $\pm$ 305	25 $\pm$ 7	296 $\pm$ 68	2.33 $\pm$ 0.33	27 $\pm$ 6

**Table 3**  
Parameters for CA release and uptake determined from signals evoked by the 120-pulse, 60-Hz train (mean  $\pm$  SE).

	Michaelis–Menten kinetics		Slope analysis	
	$V_{max}$ (nM/s)	$[CA]_p$ (nM)	$V_{max}$ (nM/s)	$[CA]_p$ (nM)
Lateral striatum	741 $\pm$ 145	31 $\pm$ 5	677 $\pm$ 109	33 $\pm$ 5
Medial striatum	936 $\pm$ 168	31 $\pm$ 6	906 $\pm$ 181	35 $\pm$ 6

stimulation sites (Garris et al., 1993), pharmacological confirmation of chemical identity (Park et al., 2010), and differences in release rates (Garris and Wightman, 1995; Capella et al., 1993). We thus performed a similar analysis of striatal signals evoked by the 24-pulse, 60 Hz train in the rat as in the starling. In general and shown in Tables 2 and 3, evoked  $[CA]_{max}$  and parameters for CA release and uptake were similar in rat and starling striata. Interestingly, both the starling and rat support high CA release and uptake rates in the striatum that appear to be more related to higher DA tissue contents than the lower NE tissue contents (see also the “Tissue monoamine content” section).

## Discussion

### Immunohistochemistry in the starling brain

DARPP-32, a marker for dopaminergic cells, was used to delineate dopaminergic regions in the starling striatum to facilitate recording electrode placement. Overall, we found that DARPP-32-IR was dense and fairly uniform throughout the MSt and LSt, which is in good agreement with previous reports in other avian species (Bálint and Csillag, 2007; Reiner et al., 1998). However, our finding that DARPP-32-IR was greatly reduced within Area X in comparison to the surrounding MSt contrasts with previous findings in the zebra finch, where Area X had equivalent (Hein et al., 2007) or slightly greater (Reiner et al., 2004) levels of DARPP-32 immunoreactivity. This result is especially surprising given the high density of D1-like receptors found in Area X in starlings (Casto and Ball, 1994), as DARPP-32 is typically present in D1 expressing neurons (Walaas and Greengard, 1984). The reason for this discrepancy is unknown. One possibility is that these changes may be due to seasonal changes in the cellular composition of Area X. In seasonally breeding songbirds, such as the European starlings, and unlike the zebra finch, the borders of Area X reduce and enlarge following the regression and recrudescence, respectively, of the gonads due to changes in neuron number and size (Ball et al., 2004; Ritters et al., 2000; Tramontin and Brenowitz, 2000). Thus, it may be possible that in Area X, DARPP-32 is a seasonally regulated gene that varies across the breeding and non-breeding seasons. However, our sampled individuals included animals in both breeding and non-breeding condition, so it seems unlikely that this apparent absence of DARPP-32 is linked to seasonal changes in Area X neurons, and we did not note any obvious sex-specific differences in DARPP-32 expression density within Area X, although Area X volume was noticeably greater in males than females as has been reported previously (Bernard et al., 1993; Ball et al., 1994). While this may merely represent a species difference in DARPP-32 expression, an additional possibility may be that DARPP-32 is reduced in the Area X of open-period song learning species. Unlike the zebra finch, which has an extremely stereotyped song (Eales, 1985), starling song is extremely variable and additional elements are added throughout a bird's lifetime (Chaiken et al., 1994; Mountjoy and Lemon, 1995). While expression of DARPP-32 has been confirmed in the striatum of the canary, another open-period learning species (Hemmings et al., 1992), expression of DARPP-32 has not been compared between Area X and the surrounding MSt in this species. Further work on this and other open-period song learning species would likely clarify whether our finding is species-specific, or representative of a subset of songbirds.

TH-IR was used to delineate the VTA, the selected target of the stimulating electrode for eliciting electrically evoked CA levels in the striatum for recording with FSCV (Fig. 2). TH is the rate-limiting enzyme in the synthesis of DA and NE and thus serves as a marker for catecholaminergic neurons. The VTA is the origin of DA neurons known to strongly project to the avian MSt including Area X, and to

a lesser extent, the LSt (Kitt and Brauth, 1986b). Similar to other songbirds such as the zebra finch (Nixdorf-Bergweiler and Bischof, 2007), and unlike the rat (Paxinos and Watson, 1986), in the starling brain, the VTA protrudes approximately 0.5 mm anterior to the substantia nigra pars compacta (SNc; see Fig. 4b and c), allowing this region to be selectively targeted for stimulating electrode placement. However, axons of passage ascending to the striatum would also be activated. Thus, if DA axons from the SNc, which innervate LSt primarily and to lesser extent the MSt (Kitt and Brauth, 1986b), and/or NE axons from locus coeruleus and subcoeruleus, which innervate Area X (Castelino et al., 2007) and other regions of the striatum (Kitt and Brauth, 1986a), pass nearby the rostral VTA, they could in theory be activated as well.

#### Monoamine content in the starling striatum

To our knowledge, no previous studies have quantified DA and NE contents of the avian striatum beyond the specialized song-learning nucleus Area X. Within Area X, DA content is at least 15-fold greater than NE content in male zebra finches (Gale and Perkel, 2005; Harding et al., 1998), similar to what we found for the starling Area X ( $\approx 10$ -fold) and MSt ( $\approx 16$ -fold). Tissue content of the entire avian anterior basal forebrain contains an approximately 10-fold difference in DA and NE levels (Juorio and Vogt, 1967), which corroborates higher DA than NE content in the starling striatum. Interestingly, DA content in the starling MSt was found to be similar to that in the rat dorsal and ventral striatum, although NE content in both the MSt and LSt appeared higher (Garris et al., 1993). Consistent with this later result, avian striata are known to receive considerably more NE innervation (as determined by immunocytochemistry) than is typical in mammalian models (Kitt and Brauth, 1986a). On the other hand, 5-HT content was highest in the posterior MSt, with only moderate levels in the hypothalamus and NAc, and consistently low levels in the anterior MSt, the LSt and Area X. The higher 5-HT content in the posterior MSt relative to the anterior MSt and the LSt of the starling is dissimilar to the relatively low but uniform levels of 5-HT content reported throughout the dorsal striatum of the rat (Beal and Martin, 1985).

Although several of the basal forebrain regions for which tissue content of monoamines is reported were not targets of *in vivo* FSCV in the current study and are not discussed in detail here, the data regarding DA:NE content in these regions may be useful in determining whether these regions are tractable for monitoring CA responses using FSCV in future studies, but should be confirmed in non-surgically manipulated birds. Additionally, pharmacological studies focusing on specific inhibition of DA and NE transporters and autoreceptors to selectively increase the DA or NE portions of the CA signal are currently underway and should provide further insight regarding the possibility of combining drug treatments with *in vivo* FSCV for monitoring potentially mixed catecholamine signals throughout the vertebrate brain.

#### Presynaptic regulation of [CA] in the starling striatum

To characterize presynaptic regulation of CA in the striatum, we electrically evoked CA release using several different stimulation regimens. [CA]<sub>max</sub> elicited by the 4-pulse, 30-Hz train ( $\approx 30$  nM) was similar to the low end of the range of naturally occurring DA transients recorded in the striatum of unanesthetized rats, whether occurring spontaneously or elicited by natural rewards and their predictive cues (Robinson et al., 2004, 2008). [CA]<sub>max</sub> elicited by the 24-pulse, 60-Hz train ( $\approx 300$  nM) was similar to the middle or high end of this range. It should be noted that urethane anesthesia blunts electrically evoked DA release in the rat (Garris et al., 1997), so quantitatively comparing stimulus trains, physiological firing patterns, and [DA] is difficult between

anesthetized and unanesthetized animals. There are only two reports of naturally occurring NE transients, which determined a maximal concentration of  $\approx 20$  to 30 nM in the bed nucleus of the stria terminalis of the rat (Park et al., 2012, 2013). While the amplitudes of these NE transients were similar to those of CA signals recorded in the starling striatum and elicited by the 4-pulse, 30-Hz train, the rate of rise appeared slower. Although data are limited, in the rat at least, NE neurons have a slower release rate than DA neurons (Garris and Wightman, 1995; Capella et al., 1993).

In contrast to the more physiologically relevant stimulations, [CA]<sub>max</sub> elicited by the 120-pulse, 60-Hz train was  $\approx 2100$  nM. This concentration is near saturating for the DA and NE transporters, which exhibit a  $K_m$  of  $\approx 200$  to 400 nM as determined by the uptake of radio-tracers into synaptosomes (Near et al., 1988; Coyle and Snyder, 1969) and *in vivo* voltammetry (Wu et al., 2001, 2002). Our results with the supraphysiological stimulation are in general agreement with those with the 24-pulse, 60-Hz trains, with the exception that the latter found a slightly greater CA release in the LSt compared to the anterior MSt while the former found no differences. This difference could be due to different stimulus parameters. Nevertheless, the general consistency across analyses supports the veracity of our CA release and uptake determinations, especially  $K_m$ , and collectively suggests similar presynaptic control of extracellular CA in the starling anterior MSt and LSt.

To date, work to characterize presynaptic regulation of extracellular CA in the avian striatum has been extremely limited. A study in a slice preparation of the zebra finch striatum using direct electrical stimulation of DA terminals and FSCV found no significant difference in the maximal amplitude of the electrically evoked DA signal ([DA]<sub>max</sub>), which is equivalent to the [CA]<sub>p</sub> used herein because a single stimulus was used to evoke DA release, or DA uptake between the MSt and LSt (Gale and Perkel, 2005), which is generally consistent with the present findings. The higher CA release rates measured here in the starling LSt compared to the anterior MSt are not consistent with the overall tissue monoamine contents reported in the "Tissue monoamine content" section and in the zebra finch striatum (Gale and Perkel, 2005), especially for DA, which suggests that the starling LSt exhibits higher CA release rates on a per terminal basis.

The  $K_m$  determined for CA uptake in the starling striatum is consistent with DA uptake by the dopamine transporter (DAT) and/or NE uptake by the norepinephrine transporter (NET) based on measurements for the rat (Coyle and Snyder, 1969; Near et al., 1988; Capella et al., 1993; Mitchell et al., 1994; Wu et al., 2001, 2002). Interestingly, DA uptake in the zebra finch measured by FSCV in a brain slice containing Area X was shown to be sensitive to NET inhibitors (Gale and Perkel, 2005). More recently, a preliminary report, based upon thorough searches of several avian genomes and expression databases, finds that the DAT ortholog is completely absent in birds (Lovell et al., 2013). Furthermore, NET is expressed in avian midbrain DA neurons as well as brain stem NE neurons, suggesting that NET is responsible for CA uptake in birds (Lovell et al., 2013). Thus, the  $K_m$  determined for CA uptake in the starling striatum is also consistent with DA uptake by NET based on affinities determined from rat synaptosomes (Raiteri et al., 1977) and expressed transporters for the human, rat, and fish (Roubert et al., 2001). Similar to its putative function in birds, in the rat cortex, NET is thought to contribute to the uptake of released DA as well as NE (Yamamoto and Novotney, 1998).

#### DA versus NE

Up until this point, we have initially and conservatively referred to signals recorded by FSCV in the starling striatum and electrically evoked by stimulation of the VTA as "CA". The question is can the chemical origin of the evoked signal be further resolved? In striatal

slices prepared from the zebra finch, electrically evoked signals recorded by *in vitro* FSCV were identified as DA based on three considerations (Gale and Perkel, 2005): (1) high DA-to-NE ratio in tissue content; (2) greater sensitivity of the CFM to DA versus NE; (3) sensitivity to pharmacological blockade of DA, but not NE, autoreceptors. No definitive identification was provided by selective inhibitors of NET, which increased the evoked signal, perhaps because DA neurons in birds may utilize NET to clear released DA (Lovell et al., 2013). Additionally, immunohistochemical studies of NE terminals in the songbird striatum using antibodies to dopamine beta-hydroxylase reveal very sparse terminal fields in the striatum (reviewed in Castellino and Schmidt, 2010). In the present study, starling striatal tissue also exhibited a similarly high DA-to-NE ratio in tissue content and the CFM was similarly more sensitive to DA than NE, both of which are consistent with the measurement of DA. Moreover, in contrast to the zebra finch slice in which the stimulating electrode potentially activates all terminals, including both DA and NE, in the vicinity of the CFM, the stimulating electrode targeting the starling VTA would only activate those NE neurons ascending to the striatum and traversing this region if this is indeed a candidate projection, which is not yet established. Thus, the nature of the electrical stimulation in the starling provides some measure of selectivity for DA, at least compared to the brain slice. In further support of the detection of DA in the starling striatum, all characteristics of the evoked signal were similar to those in the rat striatum, where the measurement of DA by FSCV is definitive (see the “Presynaptic regulation of [DA] in the rat striatum” section). Taken together, we conclude that converging evidence supports the chemical origin of the electrically evoked signal recorded in the starling striatum by FSCV as predominately DA. However, work to further characterize the potential contribution of NE to our measured signal is currently underway.

#### Summary, conclusions and future directions

This study establishes the technique of FSCV in the European starling, an avian model system, for the real-time monitoring of CA in the striatum. Coordinates targeting relevant brain regions were first identified by combining the stereotaxic placement of pins with subsequent post-mortem histological analysis of brain sections that underwent either standard histological staining or immunohistochemical labeling of either DARPP-32- or TH-immunoreactivity. These coordinates served as initial approximations that permitted stereotaxic placement of a stimulating electrode in the VTA and CFM in the MSt and LSt and were then optimized and functionally confirmed by electrically evoking and recording CA responses. To assess the likely contributions of DA and NE to the measured CA signal, CA tissue content was quantified in several subregions of the starling striatum. Finally, CA release and uptake parameters were determined from the electrically evoked signals. Taken together, our results are consistent with the measurement of electrically evoked DA levels in the starling striatum and similar presynaptic control of extracellular DA dynamics by exocytotic DA release and neuronal DA uptake in the striatum of the starling and rat.

The European starling is a desirable model system for a number of reasons. Starlings are relatively large, adaptable songbirds that tolerate captivity well, and are amenable to operant training (Gentner et al., 2004). They are common throughout much of Europe and North America and are a cavity-nesting species, which makes them highly accessible for neuroethological work (particularly *via* combining FSCV with telemetry; Garriss et al., 2004, 2007; Roham et al., 2010). Starlings are seasonal breeders and show stark differences in their hormonal and behavioral profiles both within and between the breeding and non-breeding seasons

(Williams et al., 2004), which make them a useful model of neuroendocrine interactions, such as the modulatory role of the mesolimbic dopamine system in seasonal differences in social decision-making. Given these benefits, we believe that *in vivo* FSCV will be an important tool in the study of behavioral neuroscience in the European starling.

#### Ethical statement

All experiments were performed in compliance with National Institutes of Health guidelines for the care and use of laboratory animals, and were approved by the Institutional Animal Use and Care Committee of Illinois State University.

#### Conflict of interest statement

All authors attest that no conflicts of interest exist (including financial, personal, or any other) that could inappropriately influence, or be perceived to influence, this work.

#### Authors and contributors

All authors contributed materially to the manuscript. ARS and JMC designed the study. ARS performed the experiments and analyzed the data. ARS, PAG, and JMC wrote the paper.

#### Acknowledgements

We thank Kim Garriss for technical assistance with the measurement of monoamine tissue content and Jason Hanser for statistical advice. Financial support for this work was provided by the School of Biological Sciences at Illinois State University, the Health Resources and Services Administration, U.S. Department of Health and Human Services (DHP20062), student research grants to ARS from the Animal Behavior Society and the Beta Lambda Chapter of the Phi Sigma Honor Society, and a grant from the National Institute of Drug Abuse (DA036331) to PAG.

#### References

- Bálint, E., Csillag, A., 2007. Nucleus accumbens subregions: hodological and immunohistochemical study in the domestic chick (*Gallus domesticus*). *Cell Tissue Res.* 327, 221–230.
- Ball, G.F., Auger, C.J., Bernard, D.J., Charlier, T.D., Sartor, J.J., Ritters, L.V., Balthazart, J., 2004. Seasonal plasticity in the song control system: multiple brain sites of steroid hormone action and the importance of variation in song behavior. *Ann. N.Y. Acad. Sci.* 1016, 586–610.
- Ball, G.F., Casto, J.M., Bernard, D.J., 1994. Sex differences in the volume of avian song control nuclei: comparative studies and the issue of brain nucleus delineation. *Psychoneuroendocrinology* 19, 485–504.
- Ball, G.F., Ritters, L.V., Balthazart, J., 2002. Neuroendocrinology of song behavior and avian brain plasticity: multiple sites of action of sex steroid hormones. *Front. Neuroendocrinol.* 23, 137–178.
- Banerjee, S.B., Dias, B.G., Crews, D., Adkins-Regan, E., 2013. Newly paired zebra finches have higher dopamine levels and immediate early gene Fos expression in dopaminergic neurons. *Eur. J. Neurosci.* 38, 3731–3739.
- Baur, J.E., Kristensen, E.W., May, L.J., Wiedemann, D.J., Wightman, R.M., 1988. Fast-scan voltammetry of biogenic amines. *Anal. Chem.* 60, 1268–1272.
- Beal, M.F., Martin, J.B., 1985. Topographical dopamine and serotonin distribution and turnover in the rat striatum. *Brain Res.* 358, 10–15.
- Bernard, D.J., Casto, J.M., Ball, G.F., 1993. Sexual dimorphism in the volume of song control nuclei in European starlings: assessment by a Nissl stain and autoradiography for muscarinic cholinergic receptors. *J. Comp. Neurol.* 334, 559–570.
- Berridge, C.W., 2008. Noradrenergic modulation of arousal. *Brain Res. Rev.* 58, 1–17.
- Berridge, K.C., Robinson, T.E., 1998. What is the role of dopamine in reward: hedonic impact, reward learning, or incentive salience? *Brain Res. Rev.* 28, 309–369.
- Bolhuis, J.J., Honey, R.C., 1998. Imprinting, learning and development: from behaviour to brain and back. *Trends Neurosci.* 21, 306–311.
- Capella, P., Ghasemzadeh, M.B., Adams, R.N., Wiedemann, D.J., Wightman, R.M., 1993. Real-time monitoring of electrically stimulated norepinephrine release in rat thalamus: II. Modeling of release and reuptake characteristics of stimulated norepinephrine overflow. *J. Neurochem.* 60, 449–453.

- Castelino, C.B., Diekamp, B., Ball, G.F., 2007. Noradrenergic projections to the song control nucleus area X of the medial striatum in male zebra finches (*Taeniopygia guttata*). *J. Comp. Neurol.* 502, 544–562.
- Castelino, C.B., Schmidt, M.F., 2010. What birdsong can teach us about the central noradrenergic system. *J. Chem. Neuroanat.* 39, 96–111.
- Casto, J.M., Ball, G.F., 1994. Characterization and localization of D1 dopamine receptors in the sexually dimorphic vocal control nucleus, area X, and the basal ganglia of European starlings. *J. Neurobiol.* 25, 767–780.
- Chaiken, M., Böhner, J., Marler, P., 1994. Repertoire turnover and the timing of song acquisition in European starlings. *Behaviour* 128, 25–39.
- Cheer, J.F., Heien, M.L., Garris, P.A., Carelli, R.M., Wightman, R.M., 2005. Simultaneous electrochemical and single-unit recordings in the nucleus accumbens reveal GABA-mediated responses: implications for intracranial self-stimulation. *Proc. Natl. Acad. Sci. U.S.A.* 102, 19150–19155.
- Covey, D.P., Roitman, M.F., Garris, P.A., 2014. Illicit dopamine transients: reconciling actions of abused drugs. *Trends Neurosci.* 37, 200–210.
- Coyle, J.T., Snyder, S.H., 1969. Catecholamine uptake by synaptosomes in homogenates of rat brain stereospecificity in different areas. *J. Pharmacol. Exp. Ther.* 170, 221–231.
- Daberkow, D.P., Brown, H.D., Bunner, K.D., Kraniotis, S.A., Doellman, M.A., Ragozino, M.E., Garris, P.A., Roitman, M.F., 2013. Amphetamine paradoxically augments exocytotic dopamine release and phasic dopamine signals. *J. Neurosci.* 33, 452–463.
- Day, J.J., Roitman, M.F., Wightman, R.M., Carelli, R.M., 2007. Associative learning mediates dynamic shifts in dopamine signaling in the nucleus accumbens. *Nat. Neurosci.* 10, 1020–1028.
- Doupe, A.J., Perkel, D.J., Reiner, A., Stern, E.A., 2005. Birdbrains could teach basal ganglia research a new song. *Trends Neurosci.* 28, 353–363.
- Durstewitz, D., Kröner, S., Güntürkün, O., 1999. The dopaminergic innervation of the avian telencephalon. *Prog. Neurobiol.* 59, 161–195.
- Eales, L.A., 1985. Song learning in zebra finches: some effects of song model availability on what is learnt and when. *Anim. Behav.* 33, 1293–1300.
- Flagel, S.B., Clark, J.J., Robinson, T.E., Mayo, L., Czuj, A., Willuhn, I., Akers, C.A., Clinton, S.M., Phillips, P.E., Akil, H., 2011. A selective role for dopamine in stimulus-reward learning. *Nature* 469, 53–57.
- Gale, S.D., Perkel, D.J., 2005. Properties of dopamine release and uptake in the songbird basal ganglia. *J. Neurophysiol.* 93, 1871–1879.
- Gan, J.O., Walton, M.E., Phillips, P.E., 2010. Dissociable cost and benefit encoding of future rewards by mesolimbic dopamine. *Nat. Neurosci.* 13, 25–27.
- Garris, P.A., Christensen, J.R., Rebec, G.V., Wightman, R.M., 1997. Real-time measurement of electrically evoked extracellular dopamine in the striatum of freely moving rats. *J. Neurochem.* 68, 152–161.
- Garris, P.A., Ciolkowski, E.L., Wightman, R.M., 1994. Heterogeneity of evoked dopamine overflow within the striatal and striatoamygdaloid regions. *Neuroscience* 59, 417–427.
- Garris, P.A., Collins, L.B., Jones, S.R., Wightman, R.M., 1993. Evoked extracellular dopamine in vivo in the medial prefrontal cortex. *J. Neurochem.* 61, 637–647.
- Garris, P.A., Ensman, R., Poehlman, J., Alexander, A., Langley, P.A., Sanberg, S.G., Greco, P.G., Wightman, R.M., Rebec, G.V., 2004. Wireless transmission of fast-scan cyclic voltammetry at a carbon-fiber microelectrode: proof of principle. *J. Neurosci. Methods* 140, 103–115.
- Garris, P.A., Greco, P.G., Sandberg, S.G., Howes, G., Pongmaytegl, S., Heidenreich, B.A., Casto, J.M., Ensman, R., Poehlman, J., Alexander, A., Rebec, G.V., 2007. Chapter 12: in vivo voltammetry with telemetry. In: Borland, L.M., Michael, A.C. (Eds.), *Electrochemical Methods for Neuroscience*. CRC Press, London, England, pp. 233–259.
- Garris, P.A., Wightman, R.M., 1994. Different kinetics govern dopaminergic transmission in the amygdala, prefrontal cortex, and striatum: an in vivo voltammetric study. *J. Neurosci.* 14, 442–450.
- Garris, P.A., Wightman, R.M., 1995. Regional differences in dopamine release, uptake, and diffusion measured by fast-scan cyclic voltammetry. In: Boulton, A., Baker, G., Adams, R.N. (Eds.), *Neurochemical Methods: Voltammetric Methods in Brain Systems*. Humana Press Inc, Totowa, NJ, pp. 179–220.
- Gentner, T.Q., Hulse, S.H., Ball, G.F., 2004. Functional differences in forebrain auditory regions during learned vocal recognition in songbirds. *J. Comp. Physiol. A: Sens. Neural Behav. Physiol.* 190, 1001–1010.
- Goodson, J.L., Kingsbury, M.A., 2013. What's in a name? Considerations of homologies and nomenclature for vertebrate social behavior networks. *Horm. Behav.* 64, 103–112.
- Greco, P.G., Meisel, R.L., Heidenreich, B.A., Garris, P.A., 2006. Voltammetric measurement of electrically evoked dopamine levels in the striatum of the anesthetized Syrian hamster. *J. Neurosci. Methods* 152, 55–64.
- Harding, C.F., Barclay, S.R., Waterman, S.A., 1998. Changes in catecholamine levels and turnover rates in hypothalamic, vocal control, and auditory nuclei in male zebra finches during development. *J. Neurobiol.* 34, 329–346.
- Heien, M.L.A.V., Phillips, P.E.M., Stuber, G.D., Seipel, A.T., Wightman, R.M., 2003. Overoxidation of carbon-fiber microelectrodes enhances dopamine adsorption and increases sensitivity. *Analyst* 128, 1413–1419.
- Hein, A.M., Sridharan, A., Nordeen, K.W., Nordeen, E.J., 2007. Characterization of CaMKII-expressing neurons within a striatal region implicated in avian vocal learning. *Brain Res.* 1155, 125–133.
- Hemmings Jr., H.C., Girault, J.A., Nairn, A.C., Bertuzzi, G., Greengard, P., 1992. Distribution of protein phosphatase inhibitor-1 in brain and peripheral tissues of various species: comparison with DARPP-32. *J. Neurochem.* 59, 1053–1061.
- Howard, C.D., Keefe, K.A., Garris, P.A., Daberkow, D.P., 2011. Methamphetamine neurotoxicity decreases phasic, but not tonic, dopaminergic signaling in the rat striatum. *J. Neurochem.* 118, 668–676.
- Hyland, B., Reynolds, J., Hay, J., Perk, C., Miller, R., 2002. Firing modes of midbrain dopamine cells in the freely moving rat. *Neuroscience* 114, 475–492.
- Jackson, B.P., Dietz, S.M., Wightman, R.M., 1995. Fast-scan cyclic voltammetry of 5-hydroxytryptamine. *Anal. Chem.* 67, 1115–1120.
- Juorio, A.V., Vogt, M., 1967. Monoamines and their metabolites in the avian brain. *J. Physiol.* 189, 489–518.
- Kitt, C.A., Brauth, S.E., 1986a. Telencephalic projections from midbrain and isthmal cell groups in the pigeon. I. Locus coeruleus and subcoeruleus. *J. Comp. Neurol.* 247, 69–91.
- Kitt, C.A., Brauth, S.E., 1986b. Telencephalic projections from midbrain and isthmal cell groups in the pigeon. II. The nigral complex. *J. Comp. Neurol.* 247, 92–110.
- Kristensen, E.W., Wilson, R.L., Wightman, R.M., 1986. Dispersion in flow injection analysis measured with microvoltammetric electrodes. *Anal. Chem.* 58, 986–988.
- Kubikova, L., Košťál, L., 2010. Dopaminergic system in birdsong learning and maintenance. *J. Chem. Neuroanat.* 39, 112–123.
- Kuenzel, W.J., Masson, M., 1988. *A Stereotaxic Atlas of the Brain of the Chick (Gallus domesticus)*. Johns Hopkins University Press, Baltimore, MD.
- Lovell, P.V., Carleton, J., Kisimi, B., Marzulla, T.B., Mello, C.V., 2013. Avian loss of the dopamine transporter is possibly compensated by the noradrenergic transporter in songbirds. In: Program No. 675.23. *Neuroscience 2013 Abstracts*. Society for Neuroscience, San Diego, CA, Online.
- Maney, D.L., 2013. The incentive salience of courtship vocalizations: hormone-mediated 'wanting' in the auditory system. *Hear. Res.* 305, 19–30.
- Mitchell, K., Oke, A.F., Adams, R.N., 1994. In vivo dynamics of norepinephrine release-reuptake in multiple terminal field regions of rat brain. *J. Neurochem.* 63, 917–926.
- Mountjoy, D.J., Lemon, R.E., 1995. Extended song learning in wild European starlings. *Anim. Behav.* 49, 357–366.
- Near, J.A., Bigelow, J.C., Wightman, R.M., 1988. Comparison of uptake of dopamine in rat striatal chopped tissue and synaptosomes. *J. Pharmacol. Exp. Ther.* 245, 921–927.
- Nixdorf-Bergweiler, B.E., Bischof, H.J., 2007. *A Stereotaxic Atlas of the Brain of the Zebra Finch, Taeniopygia guttata: With Special Emphasis on Telencephalic Visual and Song System Nuclei in Transverse and Sagittal Sections*. National Center for Biotechnology Information, Bethesda, MD Online.
- O'Connell, L.A., Hofmann, H.A., 2011. The vertebrate mesolimbic reward system and social behavior network: a comparative synthesis. *J. Comp. Neurol.* 519, 3599–3639.
- Palkovits, M., 1973. Isolated removal of hypothalamic or other brain nuclei of the rat. *Brain Res.* 59, 449–450.
- Park, J., Aragona, B.J., Kile, B.M., Carelli, R.M., Wightman, R.M., 2010. In vivo voltammetric monitoring of catecholamine release in subterritories of the nucleus accumbens shell. *Neuroscience* 169, 132–142.
- Park, J., Bucher, E.S., Fontillas, K., Owesson-White, C., Ariansen, J.L., Carelli, R.M., Wightman, R.M., 2013. Opposing catecholamine changes in the bed nucleus of the stria terminalis during intracranial self-stimulation and its extinction. *Biol. Psychiatry* 74, 69–76.
- Park, J., Wheeler, R.A., Fontillas, K., Keithley, R.B., Carelli, R.M., Wightman, R.M., 2012. Catecholamines in the bed nucleus of the stria terminalis reciprocally respond to reward and aversion. *Biol. Psychiatry* 71, 327–334.
- Paxinos, G., Watson, C., 1986. *The Rat Brain in Stereotaxic Coordinates*, second ed. Academic Press, New York, NY.
- Raiteri, M., Del, C.R., Bertolini, A., Levi, G., 1977. Effect of sympathomimetic amines on the synaptosomal transport of noradrenaline, dopamine and 5-hydroxytryptamine. *Eur. J. Pharmacol.* 41, 133–143.
- Ramsson, E.S., Covey, D.P., Daberkow, D.P., Litherland, M.T., Juliano, S.A., Garris, P.A., 2011. Amphetamine augments action potential-dependent dopaminergic signaling in the striatum in vivo. *J. Neurochem.* 117, 937–948.
- Reiner, A., Laverghetta, A.V., Meade, C.A., Cuthbertson, S.L., Bottjer, S.A., 2004. An immunohistochemical and pathway tracing study of the striatopallidum organization of area X in the male zebra finch. *J. Comp. Neurol.* 469, 239–261.
- Reiner, A., Perera, M., Paullus, R., Medina, L., 1998. Immunohistochemical localization of DARPP-32 in striatal projection neurons and striatal interneurons in pigeons. *J. Chem. Neuroanat.* 16, 17–33.
- Riters, L.V., 2011. Pleasure seeking and birdsong. *Neurosci. Biobehav. Rev.* 35, 1837–1845.
- Riters, L.V., Eens, M., Pinxten, R., Ball, G.F., 2000. Seasonal changes in courtship song and the medial preoptic area in male European starlings (*Sturnus vulgaris*). *Horm. Behav.* 38, 250–261.
- Robinson, D.L., Hermans, A., Seipel, A.T., Wightman, R.M., 2008. Monitoring rapid chemical communication in the brain. *Chem. Rev.* 108, 2554–2584.
- Rogers, L., 1998. Behavioral, structural and neurochemical asymmetries in the avian brain: a model system for studying visual development and processing. *Neurosci. Biobehav. Rev.* 20, 487–503.
- Roham, M., Covey, D.P., Daberkow, D.P., Ramsson, E.S., Howard, C.D., Garris, P.A., Mohseni, P., 2010. An implanted device for wireless FSCV monitoring of dopamine in an ambulatory subject. In: *Conf Proc IEEE Eng Med Biol Soc.* pp. 5322–5325.
- Roitman, M.F., Wheeler, R.A., Wightman, R.M., Carelli, R.M., 2008. Real-time chemical responses in the nucleus accumbens differentiate rewarding and aversive stimuli. *Nat. Neurosci.* 11, 1376–1377.

- Roubert, C., Sagne, C., Kapsimali, M., Vernier, P., Bourrat, F., Giros, B., 2001. A Na(+)/Cl(-)-dependent transporter for catecholamines, identified as a norepinephrine transporter, is expressed in the brain of the teleost fish medaka (*Oryzias latipes*). *Mol. Pharmacol.* 60, 462–473.
- Stamford, J.A., 1990. Fast cyclic voltammetry: measuring transmitter release in 'real time'. *J. Neurosci. Methods* 34, 67–72.
- Stokes, T.M., Leonard, C.M., Nottebohm, F., 1974. The telencephalon, diencephalon, and mesencephalon of the canary, *Serinus canaria* in stereotaxic coordinates. *J. Comp. Neurol.* 156, 337–374.
- Svec, L.A., Lookingland, K.J., Wade, J., 2009. Estradiol and song affect female zebra finch behavior independent of dopamine in the striatum. *Physiol. Behav.* 98, 386–392.
- Theunissen, F.E., Shaevitz, S.S., 2006. Auditory processing of vocal sounds in birds. *Curr. Opin. Neurobiol.* 16, 400–407.
- Tramontin, A.D., Brenowitz, E.A., 2000. Seasonal plasticity in the adult brain. *Trends Neurosci.* 23, 251–258.
- Versteeg, D.H.G., Van der Gugten, J., De Jong, W., Palkovits, M., 1976. Regional concentrations of noradrenaline and dopamine in rat brain. *Brain Res.* 113, 563–574.
- Walaas, S.I., Greengard, P., 1984. DARPP-32, a dopamine- and adenosine 3':5'-monophosphate-regulated phosphoprotein enriched in dopamine-innervated brain regions. *J. Neurosci.* 4, 84–98.
- Watson, C.J., Venton, B.J., Kennedy, R.T., 2006. In vivo measurements of neurotransmitters by microdialysis sampling. *Anal. Chem.* 78, 1391–1399.
- Wightman, R.M., Amatore, C., Engstrom, R.C., Hale, P.D., Kristensen, E.W., Kuhr, W.G., May, L.J., 1988. Real-time characterization of dopamine overflow and uptake in the rat striatum. *Neuroscience* 25, 513–523.
- Williams, T.D., Kitaysky, A.S., Vézina, F., 2004. Individual variation in plasma estradiol-17beta and androgen levels during egg formation in the European starling *Sturnus vulgaris*: implications for regulation of yolk steroids. *Gen. Comp. Endocrinol.* 136, 346–352.
- Willuhn, I., Burgeno, L.M., Groblewski, P.A., Phillips, P.E., 2014. Excessive cocaine use results from decreased phasic dopamine signaling in the striatum. *Nat. Neurosci.* 17, 704–709.
- Wu, Q., Reith, M.E., Walker, Q.D., Kuhn, C.M., Carroll, F.I., Garris, P.A., 2002. Concurrent autoreceptor-mediated control of dopamine release and uptake during neurotransmission: an in vivo voltammetric study. *J. Neurosci.* 22, 6272–6281.
- Wu, Q., Reith, M.E., Wightman, R.M., Kawagoe, K.T., Garris, P.A., 2001. Determination of release and uptake parameters from electrically evoked dopamine dynamics measured by real-time voltammetry. *J. Neurosci. Methods* 112, 119–133.
- Yamamoto, B.K., Novotney, S., 1998. Regulation of extracellular dopamine by the norepinephrine transporter. *J. Neurochem.* 71, 274–280.
- Yanagihara, S., Hessler, N.A., 2006. Modulation of singing-related activity in the songbird ventral tegmental area by social context. *Eur. J. Neurosci.* 24, 3619–3627.